Available online at www.sciencedirect.com
SCIENCE DIRECT
Journal of Sound and Vibration 295 (2006) 725–738
JOURNAL OF SOUND AND VIBRATION
www.elsevier.com/locate/jsvi

Exact solution of free in-plane vibration of a stepped circular arch

Ekrem Tufekci*, Oznur Ozdemirci

Faculty of Mechanical Engineering, Istanbul Technical University, Gumussuyu TR-34437, Istanbul, Turkey

Received 23 March 2004; received in revised form 11 October 2005; accepted 24 January 2006
Available online 11 April 2006

Abstract

This paper investigates the free in-plane vibration of stepped circular arches. The effects of axial extension, transverse shear deformation and rotatory inertia are included in the governing equations. The solution is obtained exactly by using the initial value method. The solution procedure is also applied to cases in which only one effect is considered in order to determine its contribution to the results. The results show that the aforementioned effects must be taken into account to get a better approximation to the actual behaviour of an arch, even if it is slender. The effects of step ratio, location of the step, boundary condition, opening angle and slenderness ratio on the frequency coefficients are studied. The mode transition phenomenon is also investigated and the mode shapes are given in figures. The examples in the literature are solved and comparisons are presented in the tables. Numerical solutions are obtained by using ANSYS which is a commercial finite element program. Experiments are also performed to verify the theoretical and numerical results.

1. Introduction

The arch constitutes a common structural element in many industrial fields due to its capability of transferring loads through the combined action of bending and stretching for in-plane deformations. Due to practical importance of arches, their dynamics and especially free vibrations as well as static behaviour have been studied extensively. More than 600 articles have been summarized in review articles [1–4]. In spite of the fact that many excellent papers deal with in-plane vibrations of circular arches having uniform cross-sections, there is a very limited number of studies available on the dynamic behaviour of arches of variable cross-section. This study presents an exact solution by including axial extension, shear deformation and rotatory inertia effects for in-plane free vibration of stepped circular arches.

In general, the in-plane and out-of-plane vibrations of a planar arch are coupled. However, based on the Euler–Bernoulli hypothesis, if the cross-section of arch is uniform and doubly symmetric, then the in-plane and out-of-plane vibrations are uncoupled.

It is often difficult and sometimes impossible to find general closed-form solutions for the vibration problem of a more general arch, since the governing differential equations possess variable coefficients. The exact

*Corresponding author. Tel.: +212 293 1300/2650; fax: +212 245 0795.
E-mail addresses: tufekcie@itu.edu.tr (E. Tufekci), ozdemirci@itu.edu.tr (O. Ozdemirci).

0022-460X/$ - see front matter © 2006 Elsevier Ltd. All rights reserved.
doi:10.1016/j.jsv.2006.01.048

solution of the governing equations exists only for a circular arch of uniform cross-section. The equations of free in-plane vibration of an arch become very complex when the effects of axial extension, shear deformation and rotatory inertia are taken into account. If shear deformation and rotatory inertia effects are neglected, then the equations become much simpler, but the main simplification arises if the arch axis is supposed to be also inextensible.

Laura et al. [5] used the Rayleigh–Ritz method to investigate in-plane vibration of an arch having non-uniform thickness by using the classical arch theory in which the effects of axial extension, shear deformation and rotatory inertia are neglected. Gutierrez et al. [6] studied the in-plane vibration of non-circular arches by using polynomial functions and the Ritz method. The classical arch theory was employed. Balasubramanian and Prathaph [7] developed an arch element for static and dynamic analysis of stepped circular arches by considering the axial extension and shear deformation effects. Rossi et al. [8] studied the in-plane vibrations of cantilevered non-circular arches of non-uniform cross-sections. The Ritz method with Rayleigh's optimization criteria was applied by using the classical arch theory. Finite element solutions were also obtained. Rossi and Laura [9] introduced the dynamic stiffening effect and used finite element method by considering the effects of axial extension and shear deformation. Tong et al. [10] investigated free and forced in-plane vibrations of circular arches with variable cross-sections by using the Kirchhoff assumptions in which the neutral axis is inextensible; shear deformation and rotatory inertia are neglected. The closed-form solutions for the symmetric and asymmetric stepped arches were obtained. Liu and Wu [11] applied the generalized differential quadrature rule based on Kirchhoff assumptions to solve in-plane free vibrations of circular arches with uniform, continuously varying and stepped cross-sections. Karami and Malekzadeh [12] applied the differential quadrature method to solve free vibrations of circular arches with variable cross-sections by taking into account the effects of axial extension and rotatory inertia.

The foregoing review shows that most of the researchers calculate the natural frequencies of arches with varying cross-sections by means of approximate methods such as the Galerkin method, the Rayleigh–Ritz method, cell discretization method, differential quadrature method and finite element method (FEM). The approximate results are obtained for some specific cases and boundary conditions. The Euler–Bernoulli beam theory which neglects the effects of axial extension, shear deformation and rotatory inertia is used in most of studies. With the advancement of computer technology and commercial software, the use of finite element method becomes more advantageous for complicated geometries, in the absence of any exact solution.

In the literature, the discontinuity in the cross-section of arch is considered at the crown and the effect of position of step on the frequencies is not investigated. They do not present the mode shapes.

A phenomenon of transition of modes from extensional into inextensional, which occurs at certain combinations of curvature and length of the arch has been observed by several authors [13–15]. The mode transition phenomenon is characterized by the sharp increase in frequencies of modes which is accompanied by a significant change in the mode shapes. There is still no comprehensive analysis of mode transition phenomenon and there are no proper explanations and methods for prediction the frequencies of an arch. This is possibly due to the fact that numerical simulations, commonly employed for the analyses, provide little analytical insight into the vibration problem.

In this study, the free in-plane vibration of a circular arch with discontinuously varying cross-section is investigated by using the exact solution of the equations of free vibration of a circular arch with uniform cross-section. The aim of the present study is to extend the exact solution procedure given by Tufekci and Arpaci [16] to the stepped arches. In the following, a systematic approach is presented for investigating the free vibrations of stepped circular arches. As an approximation, the arch with discontinuously varying cross-sections is divided into a number of arches with constant cross-sections. For each arch element, the governing equations given in Ref. [16] are employed and the exact solution can be obtained by extending the procedure in Ref. [16]. The overall solution of free vibration of the stepped arch can be expressed by satisfying boundary conditions at the ends and continuity and equilibrium conditions at the boundary of the adjacent elements. The effects of boundary conditions, opening angles, slenderness ratios, step ratios and position of the step on the frequency coefficients are given in diagrams. The effects of axial extension, transverse shear deformation and rotatory inertia are also considered individually. The mode shapes of the arches and the mode transition phenomenon are investigated.

2. Analysis

The governing equations of free in-plane vibrations of a circular arch with constant cross-section are given by Tufekci and Arpaci [16].

$$\begin{aligned}
\frac{\mathrm{d}w}{\mathrm{d}\phi} &= u + \frac{R}{EA}F_t, \qquad \frac{\mathrm{d}u}{\mathrm{d}\phi} = -w + \frac{RF_n}{GA/k_n} + R\Omega_b,\\
\frac{\mathrm{d}\Omega_b}{\mathrm{d}\phi} &= \frac{R}{EI_b}M_b, \qquad \frac{\mathrm{d}M_b}{\mathrm{d}\phi} = -RF_n - R\mu\frac{I_b}{A}\omega^2\Omega_b,\\
\frac{\mathrm{d}F_t}{\mathrm{d}\phi} &= F_n - R\mu\omega^2 w, \quad \frac{\mathrm{d}F_n}{\mathrm{d}\phi} = -F_t - R\mu\omega^2 u,
\end{aligned} \tag{1}$$

where u, w are the normal and tangential displacements, Ω_b is the rotation angle about the binormal axis, ϕ is the angular coordinate, R is the radius of curvature of undeformed beam axis, F_n and F_t are normal and tangential components of internal force, M_b is the internal moment about the binormal axis, E and G are Young's and shearing moduli, A is the cross-sectional area, I_b is the moment of inertia about the binormal axis, μ is the mass per unit length, k_n is the factor of shear distribution along the normal axis.

These equations can be written in matrix form as follows:

$$\frac{\mathrm{d}\mathbf{y}(\phi)}{\mathrm{d}\phi} = \mathbf{A}(\phi)\mathbf{y}(\phi), \tag{2}$$

where,

$$\mathbf{y}(\phi) = \begin{bmatrix} w \\ u \\ \Omega_b \\ M_b \\ F_t \\ F_n \end{bmatrix}, \quad \mathbf{A} = \begin{bmatrix} 0 & 1 & 0 & 0 & R/EA & 0 \\ -1 & 0 & R & 0 & 0 & Rk_n/GA \\ 0 & 0 & 0 & R/EI_b & 0 & 0 \\ 0 & 0 & -R\mu(I_b/A)\omega^2 & 0 & 0 & -R \\ -R\mu\omega^2 & 0 & 0 & 0 & 0 & 1 \\ 0 & -R\mu\omega^2 & 0 & 0 & -1 & 0 \end{bmatrix}, \tag{3}$$

The exact solution of equations is given in Ref. [16] as follows:

$$\mathbf{y}(\phi) = \mathrm{e}^{\mathbf{A}\phi}\mathbf{y}_0 \tag{4}$$

provided that the vector of initial values $\mathbf{y}_0 = \mathbf{y}(\phi_0)$, at the reference coordinate $\phi = \phi_0$, is known. The term $\mathrm{e}^{\mathbf{A}\phi}$ can be expressed exactly.

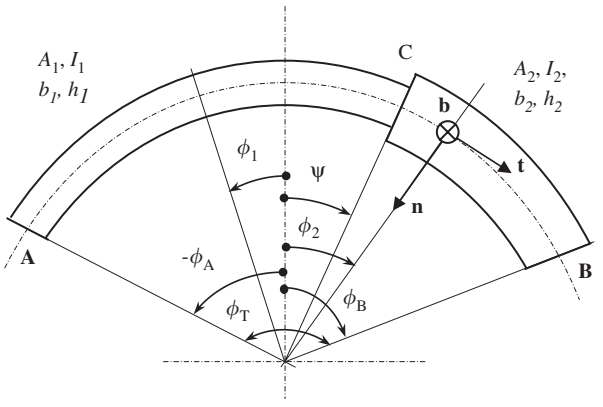

Fig. 1. Geometry of the stepped arch (**n**, **b**, **t** : right-handed coordinate axes).

The stepped circular arch given in Fig. 1 is considered in this study. This arch is divided into two parts with constant cross-sections. For each arch element, the equation of motion (1) can be written in matrix form as

$$\frac{d\mathbf{y}_1}{d\phi_1} = \mathbf{A}_1(\phi_1)\mathbf{y}_1(\phi_1), \quad -\phi_A \leqslant \phi_1 \leqslant \psi,$$

$$\frac{d\mathbf{y}_2}{d\phi_2} = \mathbf{A}_2(\phi_2)\mathbf{y}_2(\phi_2), \quad \psi \leqslant \phi_2 \leqslant \phi_B. \tag{5}$$

The exact solution of each set of equations can be found as

$$\mathbf{y}_1(\phi_1) = e^{\mathbf{A}_1\phi_1}\mathbf{y}_{01}, \quad \mathbf{y}_2(\phi_2) = e^{\mathbf{A}_2\phi_2}\mathbf{y}_{02} \tag{6}$$

provided that the vectors of initial values $\mathbf{y}_{01} = \mathbf{y}_1(\phi_{01})$, $\mathbf{y}_{02} = \mathbf{y}_2(\phi_{02})$ at the reference coordinates $\phi_1 = \phi_{01}$, $\phi_2 = \phi_{02}$ are known. The vectors of initial values must be obtained in order to specify the solution vectors $\mathbf{y}_1(\phi_1)$ and $\mathbf{y}_2(\phi_2)$. Twelve elements of the vectors can be found by using the 12 equations obtained from the boundary conditions at the ends A, B and the continuity and equilibrium conditions at point C where $\phi_1 = \psi$ and $\phi_2 = \psi$.

2.1. Boundary conditions

For end A in Fig. 1:

$$\text{Hinged end}: \quad w_1(-\phi_A) = 0, \quad u_1(-\phi_A) = 0, \quad M_{b1}(-\phi_A) = 0,$$

$$\text{Clamped end}: \quad w_1(-\phi_A) = 0, \quad u_1(-\phi_A) = 0, \quad \Omega_{b1}(-\phi_A) = 0,$$

$$\text{Free end}: \quad M_{b1}(-\phi_A) = 0, \quad F_{t1}(-\phi_A) = 0, \quad F_{n1}(-\phi_A) = 0.$$

Similar expressions are specified for the end B in Fig. 1. These conditions yield six homogeneous linear equations in terms of the initial values at reference coordinates $\phi_1 = \phi_{01}$ and $\phi_2 = \phi_{02}$.

2.2. Kinematic and kinetic continuity conditions

The continuity conditions between the adjacent domains have to be expressed. The kinematic and kinetic continuity conditions at the cross-section C, where $\phi_1 = \psi$ and $\phi_2 = \psi$, require that all quantities of both sub-domains must be equal to each other:

$$\mathbf{y}_1(\psi) = \mathbf{y}_2(\psi). \tag{7}$$

These equations can be written in such a form

$$e^{\mathbf{A}_1\psi}\mathbf{y}_{01} = e^{\mathbf{A}_2\psi}\mathbf{y}_{02}. \tag{8}$$

This also yields six simultaneous linear equations in terms of the initial values at the reference coordinates $\mathbf{y}_{01}$ and $\mathbf{y}_{02}$.

Thus, the 12 equations associated with the boundary and continuity conditions can be written in matrix form

$$\begin{bmatrix} \mathbf{X1} & \mathbf{0} \\ e^{\mathbf{A}_1\psi} & -e^{\mathbf{A}_2\psi} \\ \mathbf{0} & \mathbf{X2} \end{bmatrix} \begin{bmatrix} \mathbf{y}_{01} \\ \mathbf{y}_{02} \end{bmatrix} = [0], \tag{9}$$

where **X1** and **X2** are 3×6 matrices obtained from the boundary conditions at the ends A and B, respectively; **0**'s are 3×6 zero matrices. The determinant of the coefficient matrix of Eq. (9) must equal to zero in order to get non-trivial solution of these linear homogeneous equations. It is also possible to apply this solution procedure to other cases in which some effects are neglected.

3. Numerical evaluations and comparisons

The proposed method is applied to obtain the first five natural frequencies of the stepped arch with various boundary conditions (clamped–clamped, hinged–hinged, free–free, hinged–clamped and clamped–free). The frequency coefficients are given as $c_i = \omega_i R^2 \phi_T^2 (\mu_1/E_1 I_{b1})^{1/2}$ and calculated for five different cases which are intended to show the effects of the variation of all these geometry parameters on the frequency coefficient.

Case 1: No effect is considered (the Euler–Bernoulli arch theory in which the effects of axial extension, shear deformation and rotatory inertia are not considered).

Case 2: All effects are considered.

Case 3: Only shear deformation effect is considered.

Case 4: Only rotatory inertia effect is considered.

Case 5: Only axial extension effect is considered.

The examples are solved for all classical boundary conditions, i.e. for clamped–clamped, hinged–hinged, hinged–clamped, clamped–free and free–free end conditions. The effects of the slenderness ratio $\lambda = R/i$ (where $i = \sqrt{I/A}$ is the radius of gyration), the step ratio $\eta = h_2/h_1$, the opening angle of the arch ϕ_T, the position parameter of the step ψ/ϕ_T on the frequency coefficient are studied. The mode transition phenomenon is also studied for several configurations.

Fig. 2 shows the first frequency coefficients of a clamped–clamped arch for different cases in terms of ϕ_T and for the value of $\lambda = 50$. It can be seen that the axial extension effect is dominant. It is not possible to model the realistic arch behaviour by neglecting the axial extension effect. As it is expected, the rotatory inertia has negligible effect on the first mode. The frequency coefficient increases sharply for small opening angle and then decreases slowly for larger opening angles. The mode transition phenomenon for this arch is observed around the angle of 60°. The mode shape changes significantly from extensional into inextensional. As the slenderness ratio increases, the mode transition occurs in smaller angles. As the step ratio changes, the characteristics of the curve remain still the same for hinged–hinged, free–free and hinged–clamped boundary conditions. The figures for more slender arches or for other boundary conditions are very similar to those given in the present paper and they are not presented here for the brevity.

The frequency coefficients of a clamped–free arch are given in Fig. 3. The effects of the cases on the frequencies are shown in this figure. The axial extension has almost no influence on the frequency, and the shear deformation effect is dominant for this boundary condition, which is expected. The frequency coefficient increases as the opening angle increases. This characteristic is not observed in the frequency coefficient curves for higher modes.

The lowest five frequency coefficients of a hinged–hinged arch are given in Fig. 4. The mode transition phenomenon occurs in the opening angles in which the curves approach each other. Other boundary conditions, step ratio and position parameter do not change the characteristic of these curves.

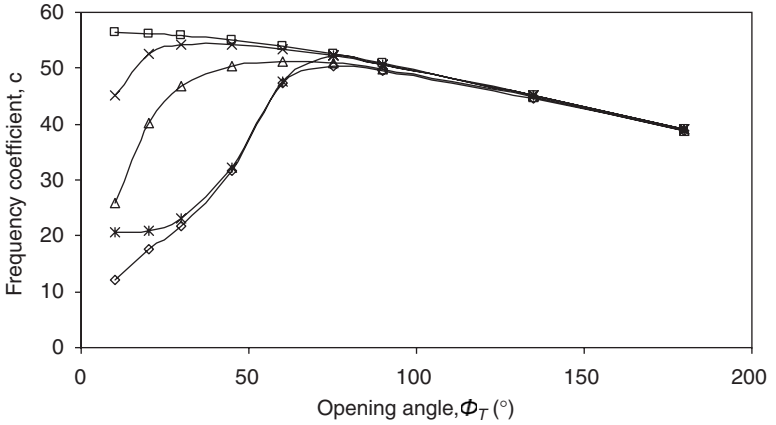

Fig. 2. The first frequency coefficient in terms of opening angle ϕ_T for a clamped–clamped arch with $\lambda = 50$, $\psi/\phi_T = 0.2$ and $\eta = 0.8$. —□—, Case 1; —◇—, Case 2; —△—, Case 3; — × —, Case 4; —*—, Case 5.

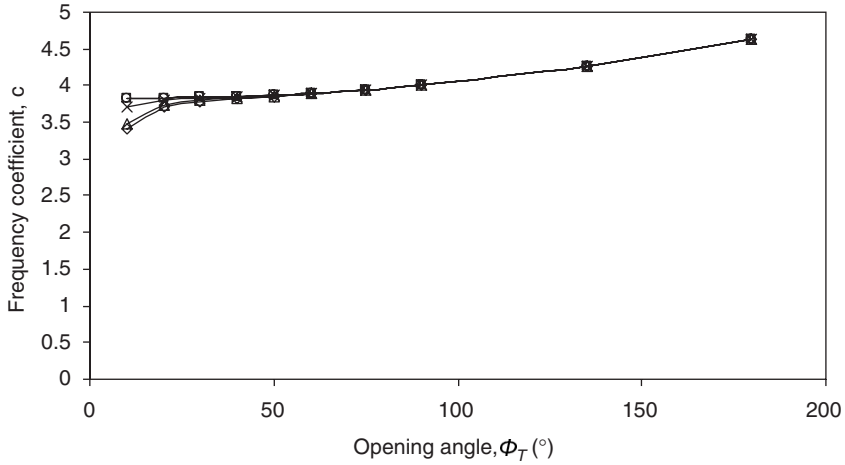

Fig. 3. The first frequency coefficient in terms of opening angle ϕ_T for a clamped–free arch with $\lambda = 50$, $\psi/\phi_T = 0.2$ and $\eta = 0.8$. —□— , Case 1; —◇—, Case 2; —△—, Case 3; — × —, Case 4; —*—, Case 5.

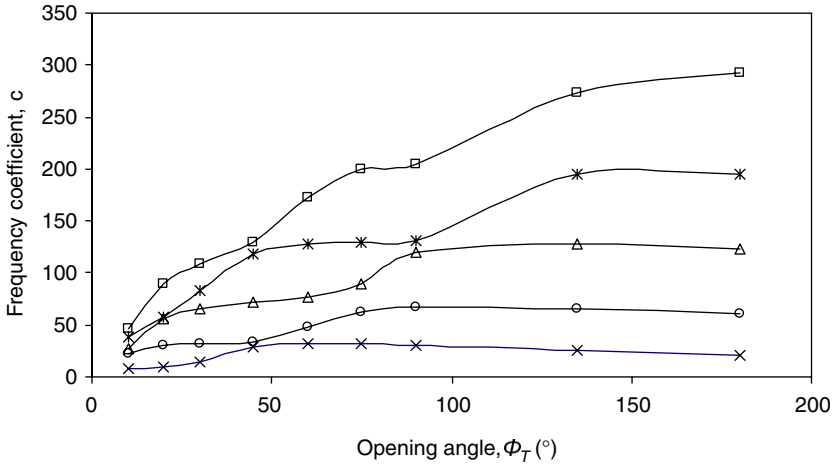

Fig. 4. The lowest five frequency coefficients in terms of opening angle ϕ_T for a hinged–hinged arch with $\lambda = 50$, $\psi/\phi_T = 0.2$ and $\eta = 0.8$. — × —, First mode; —○—, Second mode; —△—, Third mode; —*—, Fourth mode; —□—, Fifth mode.

In Fig. 5, the effects of step position on the frequency coefficients of a hinged–clamped arch are given for constant opening angles. As it can be seen in the figure, the frequency coefficient is affected slightly by the step position.

Fig. 6 gives the effect of position parameter on the frequency coefficients of a clamped–clamped arch. The similar curves are obtained for other boundary conditions except for a clamped free arch (Fig. 7). As it can be seen in Fig. 7, the frequency coefficient will be minimum for $\eta = 1.2$ and will be maximum for $\eta = 0.8$ around the position parameter of step $\psi/\phi_T = 0.1$.

Fig. 8 gives the frequency coefficients for all boundary conditions. The frequency coefficients increase sharply for small opening angles and then decrease slowly for clamped–clamped, hinged–clamped and hinged–hinged boundary conditions. But the frequency coefficients of a clamped free arch increase as the opening angle increases.

Fig. 9 shows the effect of step ratio on the frequency coefficient of a hinged–clamped arch. The frequency coefficient increases, as the step ratio increases and the slope of the curves decrease, as the position parameters of the step increase. The similar diagrams are obtained for other boundary conditions except for clamped–free

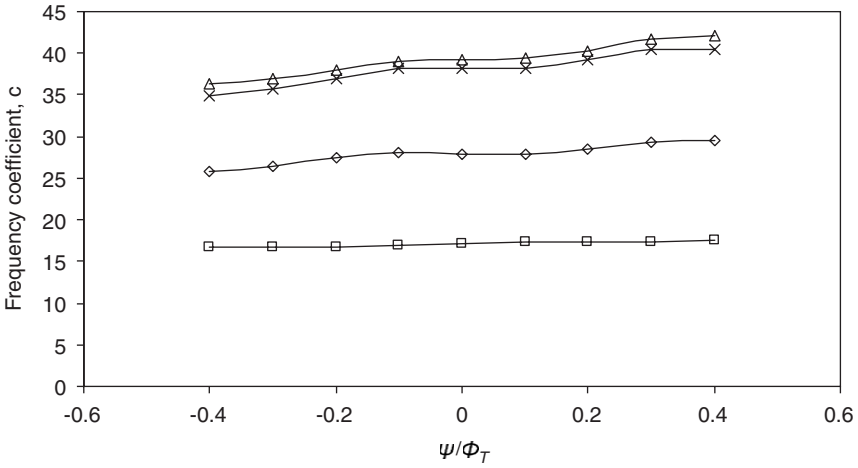

Fig. 5. The effect of step position parameter and opening angle on the first frequency coefficients for a hinged–clamped arch with $\lambda = 50$ and $\eta = 0.8$. —□—, $\phi_T = 30°$; —△—, $\phi_T = 60°$; — × —, $\phi_T = 90°$; —◇—, $\phi_T = 180°$.

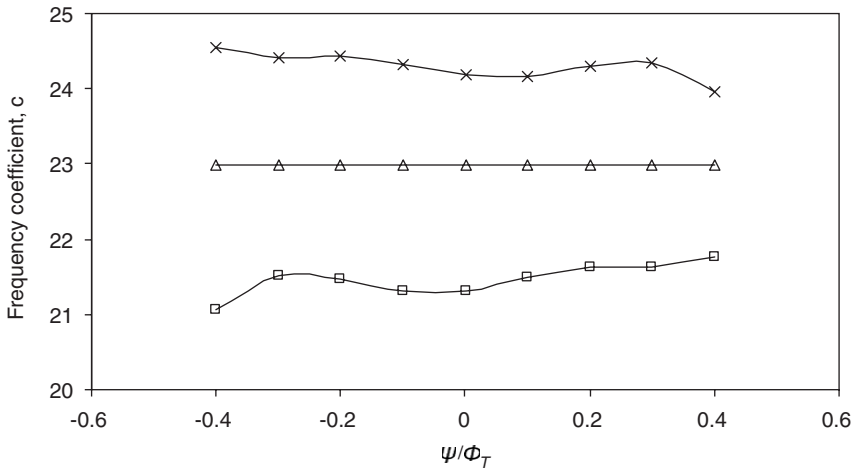

Fig. 6. The effect of step position parameter and step ratio on the first frequency coefficient for a clamped–clamped arch with $\lambda = 50$ and $\phi_T = 30°$. —□—, $\eta = 1.2$; —△—, $\eta = 1.0$; — × —, $\eta = 0.8$.

arch. In Fig. 10, the frequency coefficients are given for a clamped–free arch. The frequency coefficients are rather sensitive to the position parameter of step for all step ratios.

Fig. 11 shows the effect of step position on the first mode shape of a clamped–clamped arch with $\eta = 0.4$, $\lambda = 50$ and $\phi_T = 50°$. The mode transition from inextensional into extensional can be observed as the position parameter of step changes from 0.0 to 0.4. It is obvious that the position parameter of step can change the mode shape for such a non-shallow arch with $\phi_T = 50°$.

The first mode shapes of a clamped–clamped arch with $\eta = 0.6$, $\lambda = 50$, $\phi_T = 50°$ and $\psi/\phi_T = 0.0$ are given by neglecting all effects (case 1) in Fig. 12(a) and also by considering all effects (case 2) in Fig. 12(b). The mode shape given in Fig. 12(a) is inextensional but that in Fig. 12(b) is extensional dominant. As it can be easily seen by comparing Fig. 11 (the dotted line) and 12(b) in which the step ratios are $h = 0.4$ and 0.6, respectively, the step ratio can change the mode shape.

The following section gives the comparisons between the results of studies in the literature and those obtained in this study. In the literature, the discontinuity of arch has been considered at the crown and unsymmetrical position of step has not been investigated. Also, three boundary conditions have been

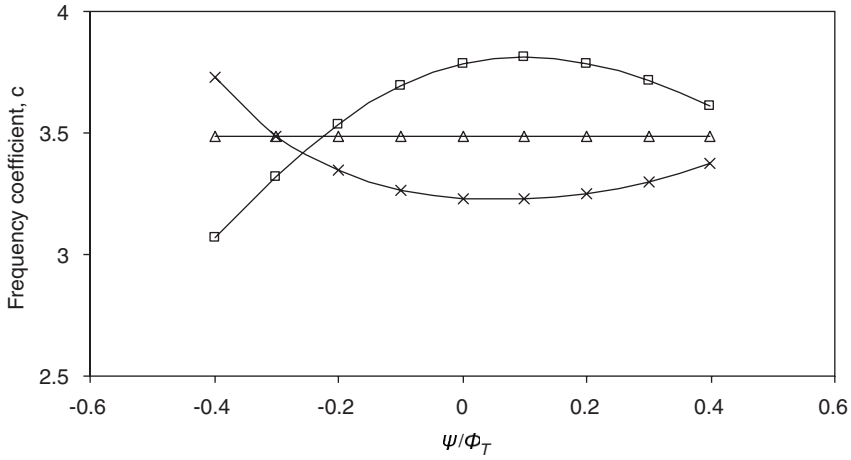

Fig. 7. The effect of step position parameter and step ratio on the first frequency coefficient for a clamped–free arch with $\lambda = 50$ and $\phi_T = 30^\circ$. —□—, $\eta = 0.8$; —△—, $\eta = 1.0$; — × —, $\eta = 1.2$.

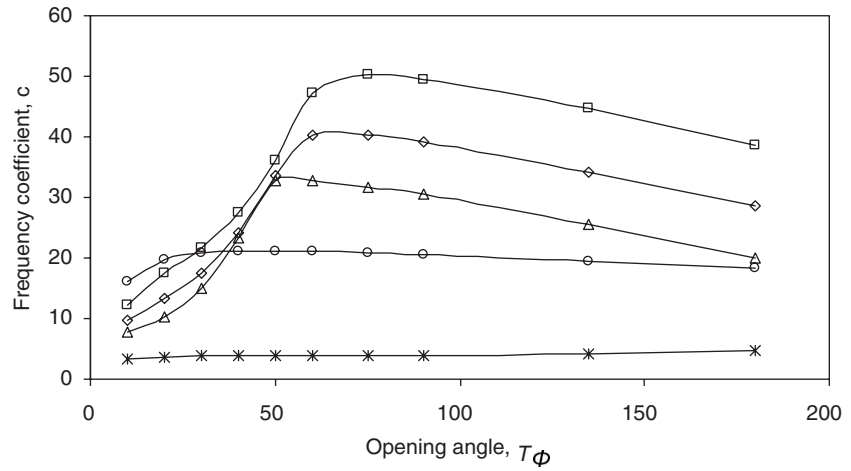

Fig. 8. The frequency coefficients of arches with different boundary conditions ($\lambda = 50$, $\eta = 0.8$ and $\psi/\phi_T = 0^\circ$). —□—, clamped–clamped; —◇—, hinged–clamped; —△—, hinged–hinged; —○—, free–free; —*—, clamped–free.

examined, clamped–clamped, hinged–hinged and hinged–clamped. In the tables, (1) and (2) give the exact solutions obtained in this study by considering no effect (case 1) and all effects (case 2) respectively.

Auciello and De Rosa [4] solved some numerical examples of stepped arches with clamped–clamped, hinged–clamped and hinged–hinged boundary conditions. The results were obtained by using the Rayleigh–Ritz (R–R), FEM and the cell discretization methods (CDM). By neglecting all effects, the first frequency coefficients $c = \omega R^2\sqrt{\mu_1/EI_1}$ were calculated for the arches with $\eta = 0.8$ and $\psi/\phi_T = 0.0$. The results are given in Table 1.

Tong et al. [10] and Liu and Wu [11] also solved the same examples to asses their solutions. The axial extension, shear deformation and rotatory inertia effects were neglected in both studies. Tong et al. [10] give the exact solution, while Liu and Wu [11] use generalized differential quadrature method and their results are given in Table 1. The exact solution of the example is obtained with and without considering all effects and the results are given in columns (1) and (2) in Table 1, respectively. The slenderness ratio is taken as $\lambda = 50$ in column (2). A very good agreement can be found between the results in the literature and those obtained in this study by neglecting all effects which are given in column (1). The results in column (2) are considerably lower than those given in column (1), since the axial extension is dominant.

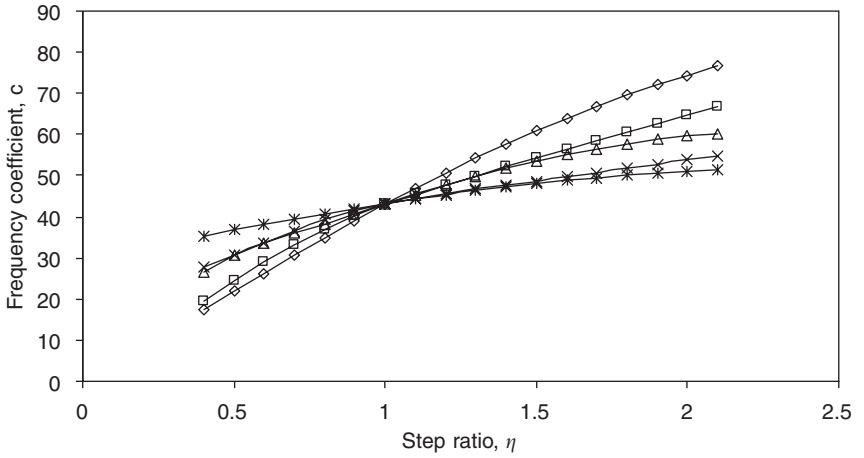

Fig. 9. The effect of step ratio on the frequency coefficients for a hinged–clamped arch with $\lambda = 50$ and $\phi_T = 90°$. —◇—, $\psi/\phi_T = -0.4$; —□—, $\psi/\phi_T = -0.2$; —△—, $\psi/\phi_T = 0.0$; — × —, $\psi/\phi_T = 0.2$; —*—, $\psi/\phi_T = 0.4$.

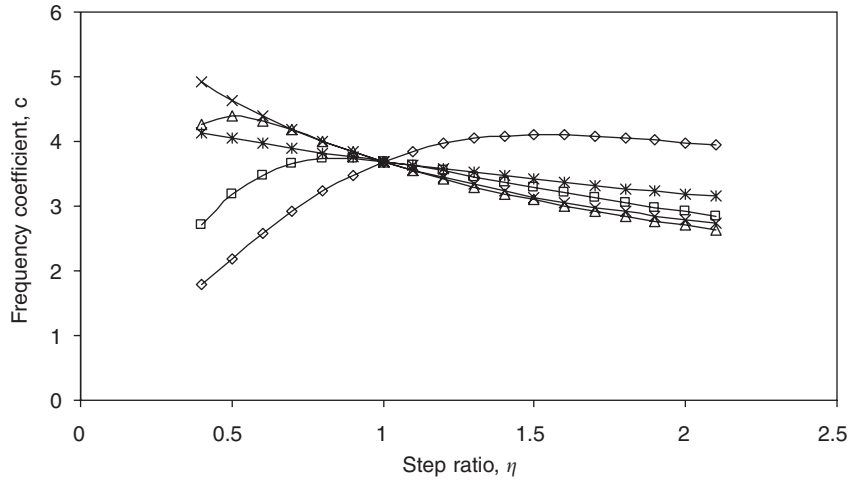

Fig. 10. The effects of step ratio η on the frequency coefficients for a clamped–free arch with $\lambda = 50$ and $\phi_T = 90°$. —◇—, $\psi/\phi_T = -0.4$; —□—, $\psi/\phi_T = -0.2$; —△—, $\psi/\phi_T = 0.0$; — × —, $\psi/\phi_T = 0.2$; —*—, $\psi/\phi_T = 0.4$.

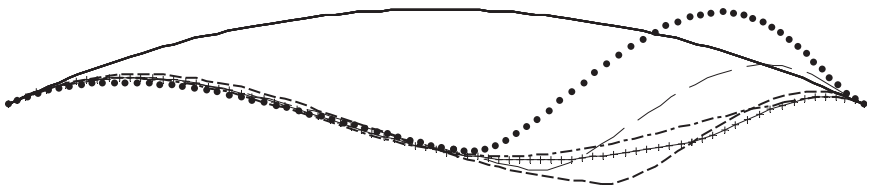

Fig. 11. The first mode shapes of clamped–clamped step circular arches with different position parameters for step ($\eta = 0.4$, $\lambda = 50$, $\phi_T = 50°$) • • •, $\psi/\phi_T = 0$; ——, $\psi/\phi_T = 0.1$; ----, $\psi/\phi_T = 0.2$; + + +, $\psi/\phi_T = 0.3$; – · – · –, $\psi/\phi_T = 0.4$.

Liu and Wu [11] calculated also the second frequency coefficients $c = \omega R^2\sqrt{\mu_1/EI_1}$ of the same arches. Table 2 shows the second frequency coefficients obtained in Ref. [11] and this study. The frequency coefficients given in column (1) are very consistent with those given in Ref. [11]. The results in column (2) are considerably lower than both those of Ref. [11] and those given in column (1). While the first frequency coefficients in columns (1) and (2) in Table 1 are satisfactorily close to each other for larger opening angles, the second

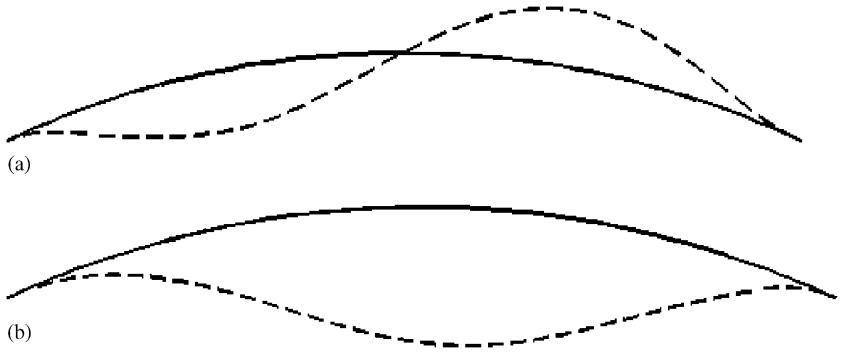

Fig. 12. The first mode shapes of a clamped–clamped step circular arch with $\eta = 0.6$, $\phi_T = 50^\circ$, $\psi/\phi = 0.0$. (a) Case 1, (b) Case 2 ($\lambda = 50$).

Table 1
The first frequency coefficients ($c = \omega R^2\sqrt{\mu_1/EI_1}$) for stepped arches ($\eta = 0.8$, $\psi/\phi_T = 0.0$): (1) no effect is considered, (2) all effects are considered ($\lambda = 50$)

ϕ_T	Ref. [4] R–R	Ref. [4] FEM	Ref. [4] CDM	Ref. [10]	Ref. [11]	(1)	(2)
Clamped–clamped							
10	2277.9	—	2264.9	2277.412	2277.436	2279.747	431.438
20	567.1	566.86	564.05	567.17	567.174	567.749	162.931
30	250.37	—	249.1	250.472	250.475	250.729	89.174
40	139.62	139.72	138.88	139.647	139.649	139.791	62.227
50	88.439	—	87.887	88.372	88.372	88.462	51.019
60	60.54	60.604	60.206	60.538	60.539	60.600	45.669
70	—	—	—	—	43.777	43.821	40.680
80	—	—	—	—	32.917	32.951	31.225
Hinged–clamped							
10	1868.5	—	1848.4	1853.663	1853.704	1855.585	363.125
20	464.76	461.15	460.03	461.342	461.352	461.820	127.893
30	205.03	—	202.95	203.52	203.525	203.731	72.164
40	114.16	113.36	112.98	113.014	113.304	113.419	54.477
50	72.103	—	71.363	71.563	71.564	71.637	47.835
60	49.269	48.978	48.775	48.91	48.911	48.961	44.119
70	—	—	—	—	35.272	35.308	33.560
80	—	—	—	—	26.439	26.466	25.449
Hinged–hinged							
10	1462.16	—	1456	1458.852	1458.838	1460.318	281.977
20	363.32	362.667	361.92	362.609	362.613	362.981	92.991
30	160.128	—	159.33	159.625	159.627	159.789	58.300
40	88.7588	88.697	88.44	88.601	88.602	88.692	49.340
50	55.8865	—	55.651	55.75	55.750	55.807	46.123
60	37.989	38.007	37.862	37.926	37.927	37.965	36.415
70	—	—	—	—	27.202	27.230	26.414
80	—	—	—	—	20.262	20.283	19.809

frequency coefficients in Table 2 are significantly different even for larger angles. This is due to the fact that the axial extension, shear deformation and rotatory inertia effects become much more important in higher modes.

Table 3 gives the first frequency coefficients $c = \omega R^2\phi_T^2\sqrt{\mu_1/EI_1}$ of arches with $\eta = 0.8$ and $\psi/\phi_T = 0.0$ for clamped–clamped, hinged–clamped and hinged–hinged boundary conditions. Gutierrez et al. [6] used polynomial functions and the Ritz method to solve in-plane vibrations of non-circular arches such as parabola, centenary, spiral and cycloid. For circular arches, the results of Ref. [6] and the present study are

Table 2
The second frequency coefficients ($c = \omega R^2\sqrt{\mu_1/EI_1}$) for stepped arches ($\eta = 0.8$, $\psi/\phi_T = 0.0$): (1) no effect is considered, (2) all effects are considered ($\lambda = 50$)

ϕ_T	Clamped–clamped			Hinged–clamped			Hinged–hinged		
	Ref. [11]	(1)	(2)	Ref. [11]	(1)	(2)	Ref. [11]	(1)	(2)
10	4027.77	4031.85	847.92	3538.34	3541.93	817.86	3054.69	3057.79	796.72
20	1005.47	1006.49	353.22	883.07	883.97	318.32	762.17	762.95	283.43
30	445.793	446.246	191.320	391.358	391.755	166.025	337.637	337.979	140.361
40	249.909	250.163	117.710	219.264	219.486	99.875	189.053	189.245	82.023
50	159.247	159.408	78.618	139.614	139.755	65.781	120.285	120.407	53.163
60	110.002	110.114	55.670	96.352	96.450	46.687	82.934	83.018	44.787
70	80.314	80.396	42.951	70.273	70.344	42.676	60.417	60.479	42.640
80	61.050	61.112	39.950	53.352	53.406	39.777	45.808	45.855	38.588

Table 3
The first frequency coefficients ($c = \omega R^2\phi_T^2\sqrt{\mu_1/EI_1}$) for stepped arches ($\eta = 0.8$, $\psi/\phi_T = 0.0$): (1) no effect is considered, (2) all effects are considered ($\lambda = 50$)

ϕ_T	Clamped–clamped			Hinged–clamped			Hinged–hinged		
	Ref. [6]	(1)	(2)	Ref. [6]	(1)	(2)	Ref. [6]	(1)	(2)
10	69.39	69.375	13.129	56.92	56.467	11.050	44.54	44.439	8.581
20	69.1	69.108	19.833	56.63	56.214	15.568	44.27	44.183	11.319
30	68.64	68.669	24.423	56.21	55.797	19.764	43.9	43.763	15.967
40	68.05	68.063	30.298	55.64	55.223	26.525	43.26	43.184	24.023
50	67.35	67.299	38.813	54.91	54.499	36.391	42.56	42.456	35.089
60	66.39	66.388	50.031	54.03	53.637	48.333	41.66	41.591	39.893

Table 4
The first frequency coefficients ($c = \omega R^2\phi_T^2\sqrt{\mu_1/EI_1}$) for stepped arch ($\phi_T = 90^\circ$, $\psi/\phi_T = 0.0$): (1) no effect is considered, (2) all effects are considered

η	Ref. [5]	(1)	(2)
1	3.7	3.697	3.691
0.8	4.01	4.013	4.007
0.6	4.32	4.321	4.315

given in Table 3. The examples are solved by excluding or including the effects in the analysis and the results are given in columns (1) and (2) respectively. By neglecting all effects, excellent agreement is obtained between the results of Ref. [6] and those obtained in this paper.

Table 4 depicts the first frequency coefficients $c = \omega R^2\phi_T^2\sqrt{\mu_1/EI_1}$ of cantilever circular stepped arch with the opening angle of $\phi_T = 90^\circ$. Laura et al. [5] obtained the results by means of the R–R method for three different values of η. All results shown in the table are very consistent, since the axial extension, transverse shear deformation and rotatory inertia effects are not so important for such a boundary condition.

4. Experimental verification

The stepped circular arches were investigated also experimentally in order to verify the theoretical results. Experiments were designed to measure the lowest few free in plane vibration frequencies on six

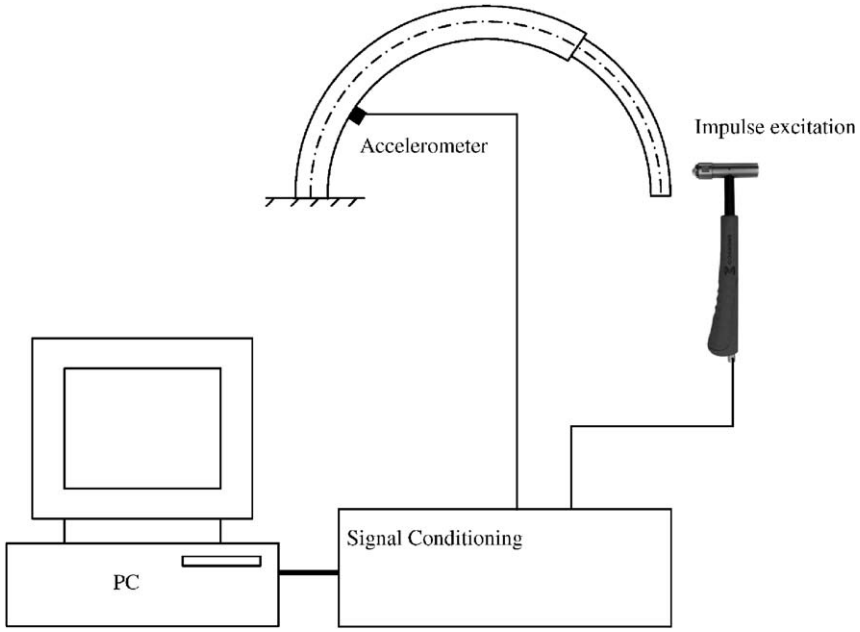

Fig. 13. Schematic view of the experimental set-up.

laboratory-scale stepped circular arches. The arch was clamped between steel blocks at the left end and free at the other end. The steel blocks were fastened with bolts to a concrete base. A rubber pad was placed between the steel support and the concrete base. The concrete base was placed on the rubber supports. The schematic view of the experimental set-up is given in Fig. 13. This design minimized the effects of vibration of the support so that the experimental frequencies of the arch could easily be identified. The arches with two different opening angles $\phi_T = 120^\circ$ and 180° and three different step positions $\psi/\phi_T = -0.2$, 0.0 and 0.2 were used in the experiments. The step ratio was chosen as $\eta = 0.8$. The arches have the same radius of curvature and cross-sectional dimensions. The radius of arch is $R = 0.20$ m. The depth of the cross-section of $b_1 = b_2 = 0.01$ m is constant and the widths are $h_1 = 0.02$ m and $h_2 = 0.016$ m at the left and right side of the step, respectively. The arches are made of steel with the nominal material properties given by $E = 2.1 \times 10^{11}$ N/m^2, $\rho = 7715$ kg/m^3, $\nu = 0.3$.

A miniature piezoelectric accelerometer (Brüel&Kjaer, type 4500) was attached to the arches in the plane of curvature in order to sense the in-plane vibrations. In a typical experiment, an impact hammer (Endevco, type 2302-10) was used to give a pulse excitation to the several points of the arch in according to the test planning. PULSE (Brüel&Kjaer) data acquisition module was used to analyse the test signals from accelerometer and hammer. The frequency range was 6 kHz. Ten measurements were performed and averaged to obtain each measured frequency. The data were transformed to frequency response functions.

Also numerical calculations were performed by using ANSYS and converged solutions based on the 3-D 20-node brick element Solid95 were obtained for two sets of opening angles $\phi_T = 120^\circ$ and 180° and three sets of position parameters of step $\psi/\phi_T = -0.2$, 0.0 and 0.2. The first six frequencies are recorded in Table 5. The results of this study and ANSYS are in an excellent agreement. Experimental results are slightly lower than the theoretical ones. Both the theoretical and numerical results are also very consistent with the measured frequencies.

5. Conclusions

This paper presents the exact solution of free in-plane vibration of stepped circular arches. The effects of axial extension, shear deformation and rotatory inertia are included in the analysis. By using the initial values method, the exact solutions are obtained in terms of the initial parameters (displacements, rotation, bending

Table 5
The natural frequencies (Hz) for clamped–free arches. Experimental, theoretical and ANSYS results

ψ/ϕ_T	$\phi_T = 120^\circ$			$\phi_T = 180^\circ$		
	Experiment	This study	ANSYS	Experiment	This study	ANSYS
−0.2	102	105.78	105.64	50	52.29	52.228
	362	388.71	389.92	140	147.89	148.20
	1212	1223.03	1224.3	472	485.49	485.98
	2442	2522.58	2531.6	1032	1073.31	1076
	3948	4071.74	4090.5	1782	1825.23	1832.2
	4918	5090.80	5094.6	2698	2735.94	2743.3
0.0	108	113.80	113.86	52	56.57	56.58
	388	405.31	405.51	144	155.10	155.14
	1268	1276.94	1282.2	486	504.88	506.43
	2484	2557.02	2562.6	1060	1087.61	1089.5
	4082	4159.28	4173.3	1828	1892.28	1899.1
	5158	5223.89	5232.5	2798	2839.25	2845.5
0.2	108	113.53	113.68	52	56.28	56.32
	432	447.71	448.67	158	171.75	172.01
	1282	1312.76	1313.1	494	521.28	521.54
	2596	2652.00	2662.6	1096	1129.44	1133.00
	4282	4341.77	4358.3	1942	1986.86	1994.10
	5128	5230.66	5241.5	2894	2963.95	2971.70

moment, shear force and normal force) at the reference coordinates. The solutions are obtained also by considering each effect individually. The effects of boundary condition, slenderness ratio, opening angle, step ratio and position parameter of step on the frequencies are investigated.

The effect of axial extension is dominant for clamped–clamped, hinged–hinged and hinged–clamped boundary conditions while the rotatory inertia has negligible effect on the first mode. The shear deformation effect is dominant for a clamped–free arch and the rotatory inertia effect is dominant for a free–free arch. For a clamped–free arch, the significantly different characteristic is observed in the first mode; the frequency coefficient increases, as the opening angle increases which is not observed in higher modes.

The frequency coefficient increases sharply for small opening angle and then decreases slowly for larger opening angles. This is due to the mode transition phenomenon from extensional into inextensional, which occurs at certain combinations of curvature and length of the arch. The mode transition phenomenon is characterized by the sharp increase in frequencies of modes which is accompanied by a significant change in the mode shapes. The mode transition phenomenon is observed around the angle in which the frequency coefficient starts to decrease. As the slenderness ratio increases, the mode transition occurs in smaller angles.

In the literature, the discontinuity of arch has been considered at the crown and the effects of the position of step on the frequencies have not been investigated. In the present study, the effects of step position on both the frequencies and the mode shapes of arches are studied. The step position affects the frequency coefficient. For certain combinations of curvature and length of the arch, the position parameter of step can also cause the mode transition.

The frequency coefficient increases, as the step ratio increases and the slope of the frequency coefficient curves decreases, as the position parameters of the step increase. For a clamped–free arch, the frequency coefficients are rather sensitive to the step position for all step ratios.

The examples in the literature are also solved. Almost all of the studies in the literature neglect the effects of axial extension, shear deformation and rotatory inertia. The solutions are obtained by using the same assumptions in the literature and a very good agreement between the results is observed. The results of the present study show that it is not possible to model the actual arch behaviour by neglecting these effects.

The experiments are performed to verify the theoretical solution. Six specimens with two different opening angles and three different step positions are used in the experiments. Only the natural frequencies are

measured. The arches are clamped at one end and free at the other end. Also the numerical results for the specimens are obtained by using ANSYS which is a commercial finite element program. 20-node brick element Solid95 is used in the numerical analysis. The converged results and the theoretical results show an excellent agreement. The measured frequencies are slightly lower than the ones computed theoretically and numerically. Both the theoretical and numerical results are also very consistent with the experimental frequencies. The differences between the experimental and theoretical frequencies are less than 8%.

The solution procedure given in the present study can provide more efficient and accurate evaluation of free vibration of stepped arches as well as a physical insight into the mode transition phenomenon.

The same investigation can be proposed for circular arches with two steps which are widely used in the practical applications. The solution procedure given in this paper can also be extended to the free vibrations of an arch with variable cross-section and variable curvature by dividing the arch into a number of stepped arches with constant radius of curvatures and uniform cross-sections.

References

[1] S. Markus, T. Nanasi, Vibration of curved beams, *The Shock and Vibration Digest* 13 (1981) 3–14.
[2] P.A.A. Laura, M.J. Maurizi, Recent research on vibrations of arch-type structures, *The Shock and Vibration Digest* 19 (1987) 6–9.
[3] P. Chidamparam, A.W. Leissa, Vibrations of a planar curved beams, rings and arches, *Applied Mechanics Reviews* 46 (1993) 467–483.
[4] N.M. Auciello, M.A. De Rosa, Free vibrations of circular arches: a review, *Journal of Sound and Vibration* 174 (1994) 433–458.
[5] P.A.A. Laura, P.L. Verniere De Irassar, R. Carnicer, R. Bertero, A note on vibrations of a circumferential arch with thickness varying in a discontinuous fashion, *Journal of Sound and Vibration* 120 (1988) 95–105.
[6] R.H. Gutierrez, P.A.A. Laura, R.E. Rossi, R. Bertero, A. Villaggi, In-plane vibrations of non-circular arches of non-uniform cross-section, *Journal of Sound and Vibration* 129 (1989) 181–200.
[7] T.S. Balasubramanian, G. Prathap, A field consistent higher-order curved beam element for static and dynamic analysis of stepped arches, *Computers & Structures* 33 (1989) 281–288.
[8] R.E. Rossi, P.A.A. Laura, P.L. Verniere De Irassar, In-plane vibrations of cantilevered non-circular arcs of non-uniform cross-section with a tip mass, *Journal of Sound and Vibration* 129 (1989) 201–213.
[9] R.E. Rossi, P.A.A. Laura, Numerical experiments on dynamic stiffening of a circular arch executing in-plane vibrations, *Journal of Sound and Vibration* 187 (1995) 897–909.
[10] X. Tong, N. Mrad, B. Tabarrok, In-plane vibration of circular arches with variable cross-sections, *Journal of Sound and Vibration* 212 (1998) 121–140.
[11] G.R. Liu, T.Y. Wu, In-plane vibration analyses of circular arches by the generalized differantial quadrature rule, *International Journal of Mechanical Sciences* 43 (2001) 2597–2611.
[12] G. Karami, P. Malekzadeh, In-plane free vibration analysis of circular arches with varying cross-sections using differential quadrature method, *Journal of Sound and Vibration* 274 (2004) 777–799.
[13] T. Tarnopolskaya, F.R. De Hoog, N.H. Fletcher, S. Thwaites, Asymptotic analysis of the free in-plane vibrations of beams with arbitrarily varying curvature and cross-section, *Journal of Sound and Vibration* 196 (1996) 659–680.
[14] T. Tarnopolskaya, F.R. De Hoog, N.H. Fletcher, Low-frequency mode transition in the free in-plane vibration of curved beams, *Journal of Sound and Vibration* 228 (1999) 69–90.
[15] E. Tufekci, Exact solution of free in-plane vibration of shallow circular arches, *International Journal of Structural Stability and Dynamics* 1 (2001) 409–428.
[16] A. Arpaci, E. Tufekci, Exact solution of in-plane vibrations of circular arches with account taken of axial extension, transverse shear and rotatory inertia effects, *Journal of Sound and Vibration* 209 (1998) 845–856.